Pergamon

Bioorganic & Medicinal Chemistry, Vol. 3, No. 3, pp. 267–277, 1995

0968-0896/95 $9.50 + .00

0968-0896(95)00021-6

Synthesis, Muscarinic Blocking Activity and Molecular Modeling Studies of 4-DAMP-Related Compounds

Maurizio Recanatini,*[a] Vincenzo Tumiatti,[a] Roberta Budriesi,[a] Alberto Chiarini,[a] Piera Sabatino,[b] Maria L. Bolognesi[a] and Carlo Melchiorre*[,a]

[a]*Department of Pharmaceutical Sciences, University of Bologna, Via Belmeloro 6, 40126 Bologna, Italy*
[b]*Department of Chemistry "G. Ciamician", Via Selmi 2, 40126 Bologna, Italy*

Abstract—A number of compounds structurally related to 4-DAMP (**1**) were synthesized and a single crystal X-ray structural study on a representative member of this series was carried out. All the compounds were tested for the antagonist activity in isolated guinea pig atria (M_2 muscarinic receptors) and ileum (M_3 muscarinic receptors). Affinity values (pA_2) for the muscarinic receptor subtypes ranged from 5.39 to 9.71 (M_2) and from 5.68 to 9.92 (M_3), depending on different structural features of the compounds. A molecular modeling study was performed, with the aim of rationalizing the affinity data for both M_2 and M_3 muscarinic receptor subtypes. The presence in the series of two highly active, structurally constrained derivatives allowed us to define two different pharmacophoric frames on which all the compounds could be fitted in a satisfactory manner.

Introduction

Muscarinic receptors have been extensively investigated during the past decade thanks to the characterization of different muscarinic receptor subtypes, which has given new impetus to the search for selective ligands for specific control of the different responses modulated by each receptor subtype. Presently, several antagonists are available which bind selectively to the pharmacologically characterized muscarinic receptors. For example, pirenzepine has high affinity for M_1 muscarinic receptors which are mainly located in the central nervous system and peripheral ganglia;[1] polymethylene tetraamines, exemplified by methoctramine and tripitramine,[2–5] display high affinity for M_2 muscarinic receptors of cardiac cells; 4-DAMP (**1**) shows high affinity for M_3 muscarinic receptors located in smooth muscle and exocrine glands.[6] Atropine, which is a classical muscarinic receptor antagonist, fails to discriminate among subtypes in both functional and binding assays.

The advent of molecular biology techniques has allowed the cloning of five muscarinic receptors (m_1–m_5).[7] m_1, m_2 and m_3 muscarinic receptors correspond to the pharmacologically defined M_1, M_2 and M_3 subtypes, respectively, whereas for m_4 and m_5 receptors the pharmacological characterization is still incomplete.

Despite the impressive results obtained with molecular biology studies, much remains to be learned about the topography of the acetylcholine or antagonist binding sites to disclose the structural requirements which determine selectivity to one receptor subtype, rather than to another. Knowledge of these parameters is inherently difficult because muscarinic receptor subtypes have more than 70% identity, which means that muscarinic ligand binding involves similar, if not identical, amino acids for different subtypes. This results in equivalent binding of most antagonists. The selectivity of **1** for M_3 muscarinic receptors serves to remind us of our ignorance about the subtle and unpredictable differences in the binding pockets that account for selectivity, because **1** apparently does not incorporate any particular structural element in its structure to which selectivity may be ascribed. In fact, **1** bears functionalities which are found in all classical and non selective antimuscarinics, that is two large hydrophobic groups α to an ester function which, in turn, are connected to a cationic head via two or three carbon atoms. Thus, the selectivity of **1** may be due to a particular conformation that it assumes in the interaction with the M_3 muscarinic receptor.

In an attempt to define the structural elements which confer muscarinic receptor subtypes selectivity, we modified the structure of **1** by incorporating its acyl portion into an oxodioxolane ring affording spiro-DAMP (**2**).[8] The study of conformationally constrained analogues of a lead compound, in which the disposition of the key groups presumably contributing to the affinity and selectivity is more or less frozen, is a useful approach when searching for clues about binding site topography. It turned out that **2** has high affinity for both M_2 and M_3 muscarinic receptors but, contrary to **1**, it was devoid of selectivity. Evidently, in spite of the fact that **2** has a conformational freedom lower than that of the flexible parent compound **1**, it may assume conformations that are capable of optimally interacting with both receptors. Now, we thought it of interest to further constrain the structure of **2** by linking together the two phenyl rings, as in **3** and **4**, to ascertain whether the relative positions of these aromatic moieties might have relevance, if any, to selectivity. With the same aim, the effect of replacing the benzylic hydrogen of **1** with other groups, such as OH, OMe, Me, Et, *n*Pr and Ph, affording **7**–**12**, was evaluated.

Furthermore, the role of the ether oxygen at the position 2' of **2** was investigated by replacing it with a sulphur atom to yield **13**.

We report here the synthesis and the biological activity in isolated guinea pig atria (M_2 muscarinic receptors) and ileum (M_3 muscarinic receptors) of compounds **3–13**, together with an X-ray structural investigation of **3** and a molecular modeling study on the whole series.

Chemistry

The structures of the compounds used in the present study are given in Table 1. These were synthesized by standard procedures and characterized by ^{1}H NMR and elemental analyses. Spiro compounds **3**, **4** and **13**[9] were synthesized through ketalization of *N*-methyl-4-piperidinone with 5-hydroxydibenzo[*a*,*d*]cycloheptadiene-5-carboxylic acid,[10] 9-hydroxy-9-fluorene-carboxylic acid and diphenyl-mercapto-acetic acid,[11] respectively, in the presence of *p*-toluenesulfonic acid as catalyst and subsequent transformation of the intermediate tertiary amines into the quaternary salts with methyl iodide. 4-DAMP (**1**) analogues **5–7**, **10** and **11** were synthesized by transforming the corresponding tertiary amines 1-methyl-4-(dibenzo[*a*,*d*]cycloheptadiene-5-carboxy)-piperidine,[12] 1-methyl-4-(fluorene-9-carboxy)-piperidine,[13] 1-methyl-4-(diphenyl-methyl)-acetyloxy-piperidine,[12] 1-methyl-4-(diphenyl-methoxy)-acetyloxy-piperidine,[12] and 1-methyl-4-(triphenyl)-acetyloxy-piperidine[12] into the quaternary salts with methyl iodide. Ethyl and *n*-propyl analogues **8** and **9** were prepared from the corresponding 2,2-diphenyl-butyric acid[14] and 2,2-diphenyl-pentanoic acid[14] which were transformed, respectively, into the acyl chloride and the methyl ester and then allowed to react with *N*-methyl-4-piperidinol. Resulting tertiary amines were converted to the corresponding methiodides with methyl iodide.

X-ray Analysis

A single-crystal X-ray crystallographic study was undertaken, in order to establish the structure of **3** and unambiguously determine its stereochemistry (Fig. 1). As in the strictly related analogue spiro-DAMP (**2**),[15] the ester

Table 1. pA_2 values in the isolated guinea pig atrium (M_2) and ileum (M_3) muscarinic receptors

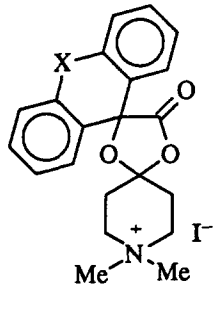

3, 4

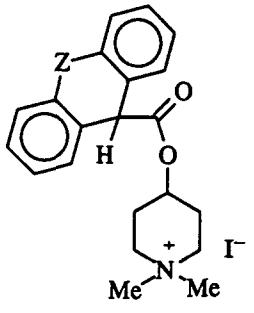

5, 6

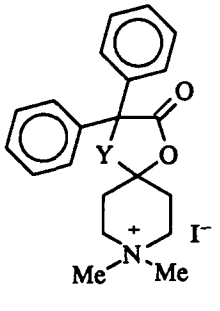

2, 13

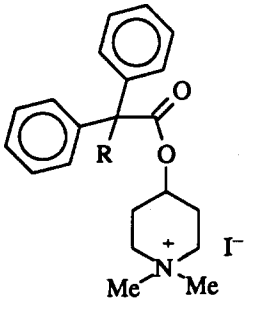

1, 7–12

no.	X	Y	Z	R	pA_2[a] M_2	M_3	selectivity[b] ratio M_3/M_2
1				H	8.53 ± 0.13	9.19 ± 0.15	4.6
2		O			8.93 ± 0.19	8.86 ± 0.10	0.8
3	CH_2CH_2				8.24 ± 0.07	8.61 ± 0.03	2.3
4	bond				5.39 ± 0.04	5.68 ± 0.04	1.9
5			CH_2CH_2		6.69 ± 0.02	6.78 ± 0.02	1.2
6			bond		8.60 ± 0.01	8.68 ± 0.08	1.2
7				Me	9.53 ± 0.09	9.92 ± 0.03	2.4
8				Et	8.16 ± 0.07	8.90 ± 0.02	5.5
9				nPr	6.70 ± 0.04	7.33 ± 0.04	4.3
10				OMe	7.57 ± 0.06	7.92 ± 0.02	2.2
11				Ph	5.75 ± 0.04	6.87 ± 0.01	13.2
12				OH	9.71 ± 0.02	9.90 ± 0.06	1.5
13		S			7.25 ± 0.01	7.83 ± 0.03	3.7

[a] pA_2 values ± SE were calculated from Schild plots,[17] constrained to slope −1.0.[18] pA_2 is the positive value of the intercept of the line derived by plotting log (DR − 1) vs log [antagonist]. The log (DR-1) was calculated at three different antagonist concentrations, and each concentration was tested at least five times. Dose–ratio (DR) values represent the ratio of the potency of the agonist carbachol (ED_{50}) in the presence of the antagonist and in its absence. Parallelism of dose–response curves was checked by linear regression, and the slopes were tested for significance ($P < 0.05$). [b]The selectivity ratio is the antilog of the difference between the pA_2 values at M_3 and M_2 muscarinic receptors.

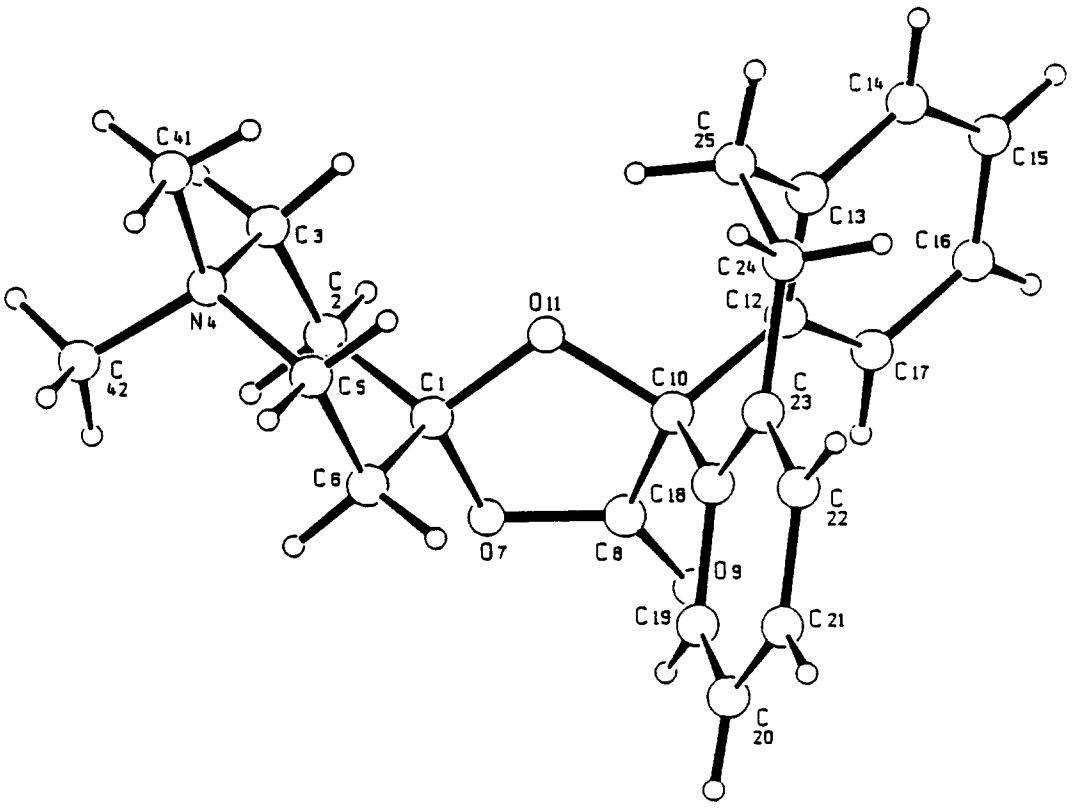

Figure 1. Molecular structure of **3** together with the crystallographic labeling; I atom has been omitted.

group of the cation is enclosed in an oxodioxolane ring, thus forming a spiro derivative. However, unlike **2** where the ester moiety is oriented in axial position, the C(1)–O(7) bond in **3** is an equatorial substituent of the piperidine ring, so that the topology of the two N(4) and O(9) atoms believed to be involved in the drug–receptor interaction is different in the two compounds.

The CH_2–CH_2 moiety bridging the two phenyl rings forms a seven-membered cycloheptadiene ring, which adopts a twist-boat conformation. Torsion angles in the latter ring exhibit the following values: C(10)–C(12)–C(13)–C(25) –8.7(5)°, C(12)–C(13)–C(25)–C(24) –65.3(5)°, C(23)–C(24)–C(25)–C(13) 60.3(5)°, C(18)–C(23)–C(24)–C(25) –6.0(5)°, C(10)–C(18)–C(23)–C(24) –1.5(5)°, C(12)–C(10)–C(18)–C(23) –50.4(5)°. The two phenyl groups form a dihedral angle of 63.3(5)°, adopting a compromise between the sterically favoured orthogonal orientation and the steric constraint exerted by the methylene bridge.

Three intramolecular H-bond interactions occur in **3**, two involving O(9) atom with C(17)–H(17) (C...O distance 2.909 Å, C–H...O angle 129.5°) and C(19)–H(19) (C...O distance 3.183 Å, C–H...O angle 124.0°) and another one involving O(11) with C(25)–H(25) (C...O distance 2.812 Å, C–H...O angle 121.9°).[16] Two interionic short contacts take place between the cation and the iodide counterion [C(5)...I, 3.885 Å and C(42)...I, 3.974 Å].

Pharmacology

The biological profile in functional experiments of compounds listed in Table 1 at peripheral muscarinic receptors was assessed by antagonism of carbachol-induced contractions of isolated guinea pig ileum (M_3 muscarinic receptors) and by antagonism of carbachol-induced inhibition of electrically stimulated guinea pig left atrium (M_2 muscarinic receptors). To allow comparison of the results, 4-DAMP (**1**), spiro-DAMP (**2**) and hydroxy-DAMP (**12**)[8] were used as the standard compounds. The biological results were expressed as pA_2 values determined from Schild plots[17] constrained to slope –1.0,[18] as required by theory. When this method was applied, it was always verified that the experimental data generated a line the derived slope of which was not significantly different from unity ($P > 0.05$).

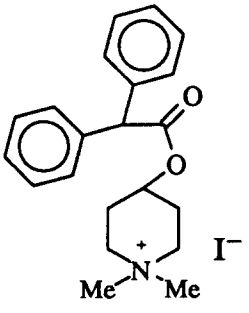

1 (4-DAMP)

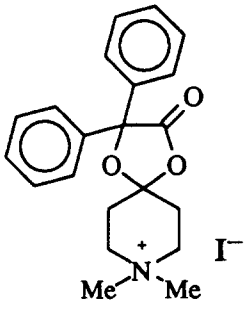

2 (spiro-DAMP)

Molecular Modeling

The semirigid and highly active molecules spiro-DAMP (**2**) and **3** were selected in order to build a pharmacophoric

frame on which to model the active conformations of the other analogues. However, the different conformations of the X-ray structures of the two spiro-compounds prompted us to carry out a conformational analysis on the piperidine ring of both of them, from which it was found that they show two major families of low energy conformations corresponding to the flipped conformations of the piperidine ring (Fig. 2). Consequently, two pharmacophores A and B were defined, which have fragments relative to the lipophilic moiety and the ester group in common, and differ with respect to the position of the ammonium N atom (Fig. 3).

The conformational search of the flexible compounds **1** and **5–12** was carried out by rotating the bonds of the intermediate ester group, while constraining selected pairs of atoms of each molecule to distances equal to those between corresponding pharmacophore's atoms. The atoms selected for constraining the search were the quaternary N atom, the ester carbonyl O atom and two dummy atoms (Du1 and Du2) calculated as centroids of the phenyl rings. The N...O, N...Du1 and N...Du2 distances of Table 2 are the mean values of the corresponding distances measured in the flipped conformations of the templates **2** and **3** from which the pharmacophoric frames were built. For each of the nine linear derivatives **1** and **5–12**, one or two conformations matching the constraining distances of the A and B templates were selected, according to criteria of best fit (rmsd) and energetic accessibility. Key interatomic distances of the 'active' conformations, the rsmd of the fit and also the ΔE values (energy difference from the estimated lowest energy conformation) for the compounds taken into consideration are reported in Tables 3 and 4.

Results and Discussion

The pA_2 values of compounds **3–13** (Table 1) cover a range of activity of about four log units, thus indicating that the structural modifications introduced in the molecule of 4-DAMP (**1**) greatly influence the biological properties of these derivatives. Linking the two phenyl rings of spiro-DAMP (**2**) with an ethyl bridge (**3**) or a direct bond (**4**) causes dramatically different effects. In fact, compound **3** retains almost the same high affinity as spiro-DAMP on both M_2 and M_3 muscarinic receptors, while compound **4** is about one thousand times less active on both subtypes. This finding indicates that, in the di-spiro compounds, the relative orientation of the phenyl rings plays a critical role in the ligand–receptor interaction. Moreover, it might also be that the ethyl bridge of **3** favorably interacts with the lipophilic cavity hosting the bulky dibenzocycloheptadiene group. The inactivity of **4** might be due to the planarity of the fluorene nucleus that, as already pointed out by Angeli *et al.*,[19] does not allow an optimal interaction with the receptor. The corresponding linear derivatives **5** and **6** behave differently, the fluorenyl analogue **6** being about two orders of magnitude more potent than the dibenzocycloheptadienyl analogue **5** on both receptor subtypes. The surprisingly high activity of **6** suggests that the flexibility of the molecule can give rise to a more productive location of the planar aromatic moiety, perhaps involving only one of the phenyl rings. In the case of **5**, it might be hypothesized that the molecule, less compact than the corresponding spiro-compound **3**, cannot optimally fit the receptor cavity. It has to be noted that in the four derivatives just discussed as well as in spiro-DAMP (**2**) the selectivity, albeit modest, of 4-DAMP is lost.

Table 2. Distances (Å) among pharmacophoric points used for constraining the search for active conformations in the linear derivatives

Pharmacophore	N...O	N...Du1	N...Du2
A	5.75	7.85	6.75
B	6.40	7.10	6.15

Table 3. Distances (Å) among pharmacophoric points of the active conformations fitting pharmacophore A

no.	N...O	N...Du1	N...Du2	rmsd[a]	ΔE[b]
1	5.45	7.87	6.99	0.21	0.0
2 (template)	5.67	7.62	6.83	0.00	0.0
3 (template)	5.74	7.74	6.60	0.00	0.0
4	5.67	7.56	7.57	0.05[c]	0.0
5	5.20	7.27	6.19	0.36	1.6
6	5.27	6.72	5.32	0.38[c]	0.0
7	5.19	6.39	5.87	0.59	0.0
8	5.36	7.23	7.54	0.42	1.1
9	5.26	7.80	7.38	0.35	1.2
10	5.22	7.87	6.99	0.37	0.0
11	5.27	7.96	6.68	0.29	0.0
12	5.49	8.11	7.27	0.36	0.0
13[d]	5.85	8.17	7.24	0.24	0.0

[a]rmsd values (Å) were calculated considering four atoms: quaternary N, carbonyl O, the centroids of the phenyl rings. [b]ΔE values (kcal mol^{-1}) are the difference between ΔH_f values (AM1) of the active and the lowest energy conformations. [c]Only one of the phenyl rings was considered in evaluating the fit. [d]Values from MNDO optimization.

Table 4. Distances (Å) among pharmacophoric points of the active conformations fitting pharmacophore B

no.	N...O	N...Du1	N...Du2	rmsd[a]	ΔE[b]
1	5.45	7.87	6.99	0.70	0.0
2 (template)	6.38	6.98	6.30	0.00	0.6
3 (template)	6.37	6.98	6.23	0.00	0.4
4	6.39	7.06	7.07	0.04[c]	0.4
5	5.20	7.27	6.19	0.59	1.6
6	5.27	6.72	5.32	0.46[c]	0.0
7	5.19	6.39	5.87	0.52	0.0
8	5.36	7.23	7.54	0.76	1.1
9	5.26	6.30	5.98	0.50	0.0
10	5.22	7.87	6.99	0.81	0.0
11	5.27	7.96	6.68	0.72	0.0
12	5.49	8.11	7.27	0.84	0.0
13[d]	6.48	7.68	7.32	0.42	1.7

[a]rmsd values (Å) were calculated considering four atoms: quaternary N, carbonyl O, the centroids of the phenyl rings. [b]ΔE values (kcal/mol) are the difference between ΔH_f values (AM1) of the active and the lowest energy conformations. [c]Only one of the phenyl rings was considered in evaluating the fit. [d]Values from MNDO optimization.

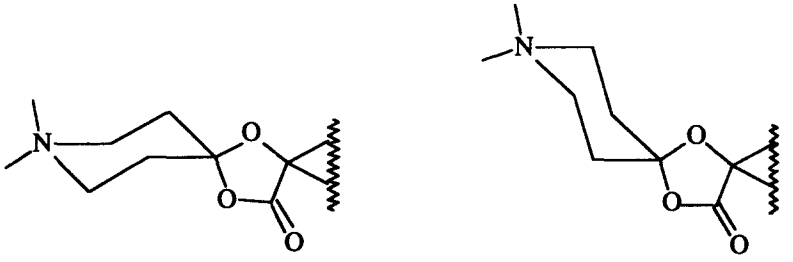

Figure 2. Representation of the two flipped conformations of the piperidine ring corresponding to low energy conformations of templates **2** and **3**.

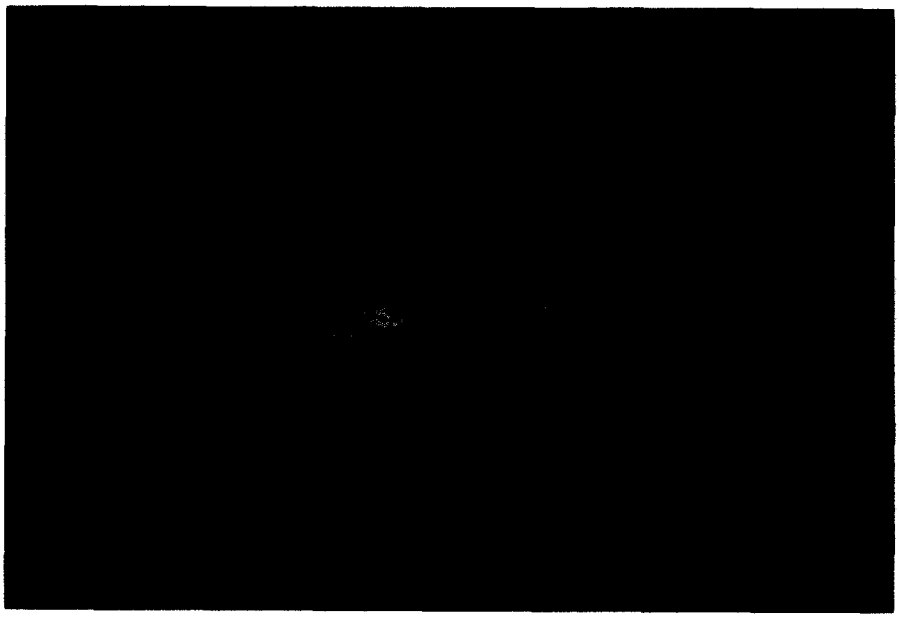

Figure 3. Superimposition of the A (red) and B (green) pharmacophoric frames onto the corresponding conformations of spiro-DAMP. Distances among the pharmacophoric points are reported in Table 2.

The substitution of the benzylic H atom of 4-DAMP led to the synthesis of the most active compounds of the series, **7** and **12**, one of which (**12**) was already known.[8] The Me (**7**) and the OH (**12**) groups caused a great increase in potency with respect to the reference compound 4-DAMP (**1**) not readily understandable in

terms of physico-chemical properties, considering that the only feature they have in common is their small size (but H is even smaller). This point will be addressed later. With regard to the other R groups (Table 1), there is a decrease of the pA_2 value in the order Et > OMe > *n*Pr > Ph at both M_2 and M_3 muscarinic receptors. The Ph-substituted derivative **11** is significantly selective towards the M_3 subtype, even if its potency is much lower than that of the most interesting compounds of the series.

Substitution of the ethereal O atom of spiro-DAMP with an S atom gave the less active compound **13** (thiospiro-DAMP). While its potency is not in the lowest range, the drop in affinity is evident at both receptor subtypes and indicates that the dioxolane ring is preferred with respect to the oxathiolane one.

From the above results, one can state that all the muscarinic antagonists **1–13** are able to bind to both M_2 and M_3 muscarinic receptors, or, in other words, that all these molecules are able to occupy the receptor cavity of either the M_2 or M_3 subtypes. In order to explain this ability shared by all the compounds, it is necessary to find a three-dimensional similarity among them in terms of

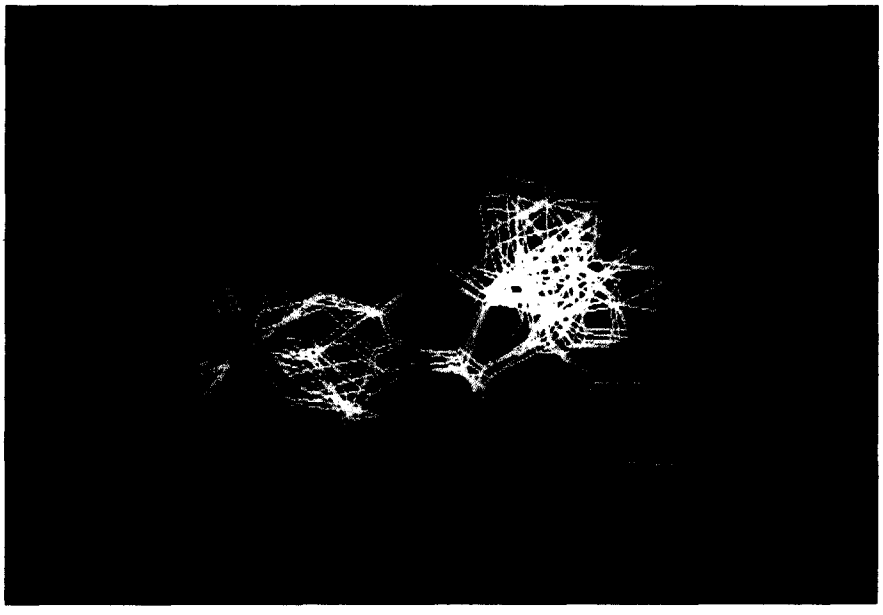

a)

b)

Figure 4. Superimposition of the 'active' conformations of all the molecules fitted to the A pharmacophore (a) and to the B pharmacophore (b). Distances among pharmacophoric points of the conformations fitting each pharmacophore are reported in Tables 3 and 4, respectively.

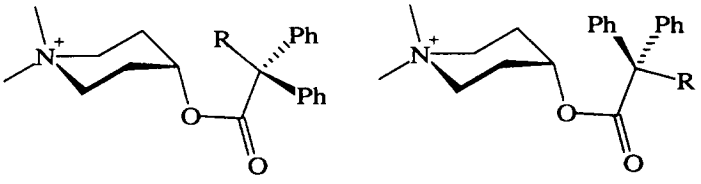

R = H, OH, OMe R = Me, Et, *n*Pr, Ph

Figure 5. Representation of the conformation assumed by α-substituted linear derivatives **1**, **10** and **12** (*endo* orientation), and **7–9** and **11** (*exo* orientation).

shape and size and also in terms of functional groups. The orientation of different ligands to the same site can be effectively obtained, provided some rigid or semi-rigid highly potent ligand is present in the series, allowing one to constrain the conformational search in the flexible derivatives.[20] In the present case, we used two templates, e.g. compounds **2** and **3**, which possess the mentioned requirements, even if they are not ideal templates, as they still display some degree of conformational flexibility. On the basis of these molecules we defined the two different pharmacophoric frames A and B which are shown in Figure 3, superimposed onto the flipped conformations of spiro-DAMP.

Given the two pharmacophores, we have found that all the compounds of the series may assume at least one accessible conformation more or less superimposable on both of them. These 'active' conformations are described by the distances among the pharmacophoric points reported in Tables 3 and 4, and are shown in Figure 4. Figures 4a and 4b show the conformations fitted to the A and to the B pharmacophores, respectively. It is noteworthy that, in most cases, the conformation of the linear molecules fitting both the templates is the same and only one.

Taking a closer look at the fitted conformations, an interesting point arises from the examination of the subset of α-substituted analogues of 4-DAMP. In these molecules (**1**, **7–12**), the benzylic substituents are oriented in different positions, according to their nature. 4-DAMP (**1**), methoxy-DAMP (**10**) and hydroxy-DAMP (**12**) assume a conformation with the benzylic H (**1**), OMe (**10**) or OH (**12**) groups oriented *endo* with respect to the piperidine ring, whereas compounds **7**, **8**, **9** and **11** orient their respective Me, Et, *n*Pr and Ph substituents *exo* with respect to the ring (Fig. 5). It might be inferred that the steric hindrance of the latter groups forces the C(carbonyl)–C(benzylic) bond to rotate in such a way as to locate the alkyl groups away from the axial hydrogen atoms of the piperidine ring. Considering that we are dealing with supposedly 'active' conformations, these orientations of functional groups might be indicative of some possible additional binding subsites.

Methyl, ethyl, propyl and phenyl groups of **7**, **8**, **9** and **11**, respectively, may occupy a lipophilic pocket or, more probably, fill part of the cavity occupied by the two phenyl rings. Considering the pA_2 values of α-substituted compounds at M_2 and M_3 muscarinic receptors (Table 1), it appears that the Me group of **7** gains the optimal occupation of the lipophilic cavity, and that further increasing the size of the substituent leads to a decrease in affinity for both receptor sites. Interestingly, in the series Me (**7**), Et (**8**), *n*Pr (**9**) and Ph (**11**), the pA_2 values for both receptor subtypes show a negative trend that appears linearly correlated with the length parameter L.[21] The correlation coefficients are 0.986 for the M_2 and 0.961 for the M_3 data, respectively.

Turning to methoxy-DAMP (**10**) and hydroxy-DAMP (**12**), it seems reasonable that their respective OMe and OH groups do not interact with the same lipophilic cavity just discussed for the other α-substituted derivatives, but broadly fall in the same space occupied by the ethereal O atom of the spiro-derivatives (Fig. 4). Also, the S atom of thiospiro-DAMP (**13**) occupies the same space. Although the area occupied by the above mentioned polar functions is not precisely defined, the very high affinity of **12** for both receptor subtypes implies an additional strong interaction, possibly due to a hydrogen bond formation with a donor residue on the receptor. The fact that the spiro-derivatives have lower affinity than the hydroxy analogue of 4-DAMP suggests that the position of the ethereal O of the templates is not ideal. Moreover, the methoxy-derivative **10** shows decreased affinity with respect to the OH analogue, probably because of the presence of the methyl group hindering the O atom or even colliding with the donor residue on the receptor. Affinity values of thiospiro-DAMP (**13**) are lower than those of spiro-DAMP (**2**), because of the lower ability of S to act as an H-bond acceptor.

In conclusion, we have synthesized and tested a number of derivatives of 4-DAMP, some of which are active in the nanomolar range. Starting from low energy conformations of two partially rigid highly potent molecules, we built two pharmacophoric frames, A and B (Fig. 3), able to account for the receptor binding of all the members of the series.

Experimental

Chemistry

Melting points were taken in glass capillary tubes on a Büchi SMP-20 apparatus and are uncorrected. IR and ^{1}H NMR spectra were recorded on Perkin–Elmer 297 and Varian VXR 300 instruments, respectively. Chemical shifts are reported in parts per million (ppm) relative to tetramethylsilane (TMS), and spin multiplicities are given as *s* (singlet), *d* (doublet), *t* (triplet), *q* (quartet) or *m*

(multiplet). Although the IR spectra data are not included (because of the lack of unusual features), they were obtained for all compounds reported and were consistent with the assigned structures. The elemental compositions of the compounds agreed to within ±0.4% of the calculated value. The term 'dried' refers to the use of anhydrous sodium sulfate.

1",1"-Dimethyl-5'-oxo-dispiro[dibenzo[a,d]cycloheptadiene-5,4'-dioxolane-2',4"-piperidinium] iodide (3). A mixture of 5-hydroxydibenzo[*a*,*d*]cycloheptadiene-5-carboxylic acid[10] (2.4 g, 10 mmol), 1-methyl-4-piperidinone (1.14 g, 9.8 mmol) and *p*-toluenesulfonic acid (1.90 g, 10 mmol) in anhydrous benzene (50 mL) was heated under reflux and the water formed continuously removed for 36 h. The cooled (*ca* 5 °C) mixture was made basic with a 10% Na_2CO_3 solution; the organic layer was removed and the aqueous phase was extracted with benzene (3 × 30 mL). The organic extracts were combined and washed with a saturated NaCl solution (2 × 15 mL). Removal of the dried solvent gave a residue which was dissolved in methylene chloride (5 mL) and treated with an excess of methyl iodide (5.4 mL). The resulting solution was left overnight in a refrigerator; the precipitated crystals were collected and recrystallized to give **3** in 37% yield: mp 192–193 °C (from EtOH); ^{1}H NMR (DMSO-d_6) δ 7.62–7.20 (8, *m*), 3.56–3.41 (6, *m*), 3.32–3.10 (8, *m*), 2.35–2.02 (4, *m*). Anal. ($C_{23}H_{26}INO_3$) C, H, N.

1",1"-Dimethyl-5'-oxo-dispiro[9H-fluorene-9,4'-dioxolane-2',4"-piperidinium] iodide (4). This was synthesized in 44% yield from 9-hydroxy-9-fluorenecarboxylic acid following the procedure described for **3**: mp 280 °C dec, (from EtOH); ^{1}H NMR (DMSO-d_6) δ 7.92–7.39 (8, *m*), 3.75–3.62 (4, *m*), 3.30 (3, *s*), 3.22 (3, *s*), 2.85–2.55 (4, *m*). Anal. ($C_{21}H_{22}INO_3 \cdot 3H_2O$) C, H, N.

2-Oxo-3,3-diphenyl-8,8-dimethyl-1-oxa-4-thia-8-azonia-spiro[4,5]decane iodide (13). This was synthesized in 25% yield from diphenyl-mercapto-acetic acid[11] following the procedure described for **3**: mp 280–281 °C (from EtOH); ^{1}H NMR (DMSO-d_6) δ 7.45–7.25 (10, *m*), 3.55–3.35 (4, *m*), 3.15 (3, *s*), 3.05 (3, *s*), 2.71–2.55 (2, *m*), 2.20–2.05 (2, *m*). Anal. ($C_{21}H_{24}INO_2S$) C, H, N.

1,1-Dimethyl-4-(dibenzo[a,d]cycloheptadiene-5-carboxy)-piperidinium iodide (5). A solution of 1-methyl-4-(dibenzo[*a*,*d*]cycloheptadiene-5-carboxy)-piperidine[12] (5 mmol) in acetone (5 mL) was treated with an excess of methyl iodide and left overnight in a refrigerator. The precipitated crystals were collected and recrystallized to give **5** in 70% yield: mp 211–213 °C (from EtOH/2-PrOH); ^{1}H NMR (DMSO-d_6) δ 7.45–7.11 (8, *m*), 5.18 (1, *s*), 4.98–4.82 (1, *m*), 3.41–2.72 (14, *m*), 2.22–1.95 (2, *m*), 1.85–1.65 (2, *m*). Anal. ($C_{23}H_{28}INO_2$) C, H, N.

1,1-Dimethyl-4-(fluorene-9-carboxy)-piperidinium iodide (6). This was obtained in 70% yield from 1-methyl-4-(fluorene-9-carboxy)-piperidine[13] following the procedure described for **5**: mp 133–135 °C (from EtOH/2-PrOH); ^{1}H NMR (DMSO-d_6) δ 7.95–7.25 (8, *m*), 5.08 (1, *s*), 4.92–4.81 (1, *m*), 3.55–3.22 (4, *m*), 3.18–2.85 (6, *m*), 2.25–1.65 (4, *m*). Anal. ($C_{21}H_{24}INO_2$) C, H, N.

1,1-Dimethyl-4-(diphenyl-methyl)-acetyloxy-piperidinium iodide (7). This was obtained in 65% yield from 1-methyl-4-(diphenyl-methyl)-acetyloxy-piperidine[12] following the procedure described for **5**: mp 197–200 °C (from Et_2O/2-PrOH); ^{1}H NMR (DMSO-d_6) δ 7.45–7.15 (10, *m*), 5.05–4.95 (1, *m*), 3.42–3.33 (2, *m*), 3.25–2.92 (8, *m*), 2.20–2.05 (2, *m*), 1.95–1.75 (5, *m*). Anal. ($C_{22}H_{28}INO_2$) C, H, N.

1,1-Dimethyl-4-(diphenyl-methoxy)-acetyloxy-piperidinium iodide (10). It was obtained in 70% yield from 1-methyl-4-(diphenyl-methoxy)-acetyloxy-piperidine[12] following the procedure described for **5**: mp 214–215 °C (from MeCOMe/2-PrOH); ^{1}H NMR (DMSO-d_6) δ 7.45–7.31 (10, *m*), 5.05–4.95 (1, *m*), 3.40–3.25 (2, *m*), 3.15–2.85 (11, *m*), 2.15–2.02 (2, *m*), 1.90–1.75 (2, *m*). Anal. ($C_{22}H_{28}INO_3$) C, H, N.

1,1-Dimethyl-4-(triphenyl)-acetyloxy-piperidinium iodide (11). It was obtained in 65% yield from 1-methyl-4-(triphenyl)-acetyloxy-piperidine[12] following the procedure described for **5**: mp 248–249 °C (from Et_2O/2-PrOH); ^{1}H NMR (DMSO-d_6) δ 7.45–7.11 (15, *m*), 5.12–5.02 (1, *m*), 3.30–3.20 (2, *m*), 2.97 (3, *s*), 2.84 (3, *s*), 2.65–2.52 (2, *m*), 2.15–2.02 (2, *m*), 1.85–1.71 (2, *m*). Anal. ($C_{27}H_{30}INO_2$) C, H, N.

1,1-Dimethyl-4-(diphenyl-ethyl)-acetyloxy-piperidinium iodide (8). A solution of 2,2-diphenylbutyric acid[14] (1.0 g, 4.1 mmol) and $SOCl_2$ (5 mL) was heated under reflux for 2 h. Removal of the excess of $SOCl_2$ gave a residue that was dissolved in anhydrous benzene (10 mL) and then added, with cooling, to a solution of 1-methyl-4-piperidinol (0.43 g, 3.7 mmol) and triethylamine (0.6 mL, 4.3 mmol) in anhydrous benzene (10 mL). The resulting mixture was heated under reflux for 2 h and then left overnight at room temperature with stirring. Removal of washed (H_2O and saturated aqueous $NaHCO_3$) and dried solvents afforded a residue that was dissolved in acetone (2 mL) and treated with an excess of methyl iodide. Resulting solution was left overnight in a refrigerator; the precipitated crystals were collected and recrystallized to give **8**: 10% yield; mp 224–226 °C (from 2-PrOH/Et_2O); ^{1}H NMR (DMSO-d_6) δ 7.40–7.15 (10, *m*), 4.98–4.90 (1, *m*), 3.35–3.20 (2, *m*), 2.99 (3, *s*), 2.94 (3, *s*) 2.88–2.75 (2, *m*), 2.38 (2, *q*, J = 7 Hz), 2.15–2.01(2, *m*), 1.81–1.65 (2, *m*), 0.66 (3, *t*, J = 7 Hz). Anal. ($C_{23}H_{30}INO_2$) C, H, N.

1,1-Dimethyl-4-(diphenyl-n-propyl)-acetyloxy-piperidinium iodide (9). A solution of 2,2-diphenyl-pentanoic acid[14] (1.35 g; 5.3 mmol) and concentrated H_2SO_4 (2 mL) in dry methanol (40 mL) was heated under reflux for a week. The solvent was removed under reduced pressure, the residue was dissolved in chloroform and washed with water (3 × 20 mL), 2.5% Na_2CO_3 (3 × 20 mL) and water (3 × 20 mL). Removal of dried (Na_2SO_4) solvents gave 0.9 g of crude methyl 2,2-diphenyl-pentanoate. A solution of this ester (0.75 g, 2.8 mmol) in anhydrous benzene (5 mL)

was added to a solution of *N*-methyl-4-piperidinol (0.7 g, 6 mmol) and NaH (0.3 g, 12 mmol) in anhydrous benzene (20 mL). The resulting mixture was heated to reflux for 4 h, then, after cooling, it was washed several times with water. Removal of dried (Na_2SO_4) solvents gave a residue which was dissolved in methylene chloride (10 mL) and treated with an excess of methyl iodide (2.5 mL). The resulting solution was left overnight in a refrigerator; the precipitated crystals were collected and recrystallized to give **9**: 15% yield; mp 239–242 °C (from 2-PrOH/Et_2O); ^{1}H NMR (DMSO-d_6) δ 7.40–7.21 (10, *m*), 4.98–4.90 (1, *m*), 3.32–3.21 (2, *m*), 2.99 (3, *s*), 2.94 (3, *s*) 2.88–2.75 (2, *m*), 2.35–2.27 (2, *m*), 2.15–1.98 (2, *m*), 1.81–1.65 (2, *m*), 1.05–0.95 (2, *m*), 0.84 (3, *t*, *J* = 6 Hz). Anal. ($C_{24}H_{32}INO_2$) C, H, N.

X-Ray crystallography

Single-crystal X-ray data for **3**, $C_{23}H_{26}INO_3$, M_r 491.35, were determined from a yellow transparent crystal, obtained from ethanol, of 0.35 × 0.51 × 0.42 mm in size.[22] The crystal belongs to the monoclinic space group $P2_1/c$, with a = 14.807(3), b = 11.524(2), c = 12.575(4) Å, β = 103.16(2)°, V = 2089(1) Å^3, Z = 4, $D_{calc.}$ = 1.52 g cm^{-3}. A total of 3568 reflections were collected at room temperature between 2.5 ≤ θ ≤ 25° using monochromatized Mo Kα radiation (λ = 0.71069 Å) by the ω-2θ scan technique on an Enraf–Nonius CAD4 diffractometer. The structure was solved by direct methods[23] and subsequent difference Fourier maps and refined by full-matrix least-squares methods[24] on F^2, using 3059 independent reflections with $I > 2\sigma I$ to a final R of 0.026 (wR^2 = 0.081). No absorption correction was applied (μ = 1.55 mm^{-1}).

All non-hydrogen atoms were allowed to vibrate anisotropically. The majority of the hydrogen atoms were located from difference Fourier maps, while the remaining ones were geometrically positioned and refined "riding" on their respective C atom with adequate constraints. The maximum and minimum difference electron density residuals at the end of the refinement were 0.63 and –0.60 eÅ^{-3}, respectively, on the proximity of the iodine atom.

Pharmacology

Guinea pigs (200–400 g) were sacrificed by cervical dislocation under ketamine anaesthesia and the organs required were set up rapidly under a suitable resting tension in 15 mL organ baths containing physiological salt solution kept at appropriate temperature (see below) and aerated with 5% CO_2–95% O_2 at pH 7.4. Dose–response curves were constructed by cumulative addition of the agonist. The concentration of agonist in the organ bath was increased approximately five-fold at each step, with each addition being made only after the response to the previous addition had attained a maximal level and remained steady. Contractions were recorded by means of a force displacement transducer (FT.03 Grass and 7003 Basile) connected to a four-channel pen recorder (Battaglia–Rangoni KV 380). In all cases, parallel experiments in which tissues did not receive any antagonist were run in order to check any variation in sensitivity.

Functional antagonism in left atria

The heart of guinea pigs of either sex was rapidly removed, washed by perfusion through the aorta with oxygenated physiological salt solution and right and left atria were separated out. The left atria were mounted under 0.2–0.3 g tension at 37 °C in Tyrode solution of the following composition (mM): NaCl, 136.9; KCl, 5.4; $MgSO_4 \cdot 7H_2O$, 1.0; $CaCl_2$, 2.52; NaH_2PO_4, 0.4; $NaHCO_3$, 11.9; glucose, 5.5. Tissues were stimulated through platinum electrodes by square-wave pulses (0.6–0.8 msec, 1 Hz, 1–5 V). Inotropic activity was recorded isometrically. Tissues were equilibrated for 1 h, and cumulative dose–response curves to carbachol (0.01–1 μM) were constructed. Following incubation with the antagonist for 30 min, a new dose–response curve to carbachol was obtained.

Functional antagonism in ileum

The terminal portion of the ileum was excised after discarding the 8–10 cm nearest to the ileo-caecal junction. The tissue was cleaned and segments of approximately 2 cm were set up under 1 g tension at 37 °C in organ baths containing Tyrode solution of the following composition (mM): NaCl, 118; KCl, 4.75; $CaCl_2$, 2.54; $MgSO_4$, 1.2; $KH_2PO_4 \cdot 2H_2O$, 1.19; $NaHCO_3$, 25; glucose, 11. Tension changes were recorded isotonically. Tissues were allowed to equilibrate for at least 30 min during which time the bathing solution was changed every 10 min. Dose–response curves to carbachol (0.01–0.5 μM) were obtained at 30 min intervals, the first one being discarded and the second one taken as control. Following incubation with the antagonist for 30 min, a new dose–response curve to the agonist was obtained.

Determination of dissociation constants

The antagonist potency of compounds listed in Table 1 at M_2 and M_3 muscarinic receptor subtypes was expressed in terms of their pA_2 values. pA_2 values were estimated by Schild plots[17] constrained to slope –1.0,[18] as required by the theory, by calculating the ratio of the doses (DR) of agonist causing 50% of the maximal response in the presence and in the absence of the test compound. The log(DR – 1) was calculated at three antagonist concentrations, and each concentration was tested at least five times. When applying this method, it was always verified that the experimental data generated a line the derived slope of which was not significantly different from unity ($P > 0.05$).

Data are presented as means ± S.E. of *n* experiments. Differences between mean values were tested for significance by the Student's *t*-test, and a level of $P < 0.05$ was taken as being statistically significant.

Molecular modeling

Molecular modeling was performed by means of the SYBYL software[25] running on a VAXStation 3100 (Digital Equipment Corporation); the graphic models were studied on an IBM PC PS/VP 450DX2, using the program NITRO[26] as a graphic interface to SYBYL.

Crystal coordinates were entered via the CRYSIN command and used as starting geometries whenever possible; all compounds were studied as quaternary ammonium derivatives. X-Ray structures of **2** and **3** were initially minimized with the Tripos force field (MAXIMIN2), without taking into consideration the electrostatic charges. Then each flexible ring of both molecules was subjected to a conformational search separately, i.e. while keeping the other(s) fixed. The oxodioxolane ring was studied first, then the piperidine ring, then the dibenzocycloheptadienic nucleus of **3**. Within the SEARCH procedure, increments of 3° over the range 0–360° were given to each rotatable bond. For both compounds it resulted that the lowest energy conformation showed a geometry fully superimposable to that of the crystal structure. However, each derivative showed a family of conformations with the piperidine ring flipped with respect to the starting geometry and in both cases the lowest energy conformations of each family showed close energy values (< 1.0 kcal mol^{-1}, Tripos force field).

Compounds **1** and **4–13** were first analyzed in order to locate low energy conformations. With regard to the linear derivatives **1** and **5–12**, 'portions' of the molecules were studied separately, due to the high number of rotatable bonds. As the starting geometry of **1** (4-DAMP) and of **12** (hydroxy-DAMP), the respective crystal structures were used,[15,27] while all other linear derivatives were built by properly modifying the X-ray structure of 4-DAMP. The geometry of the tricyclic nucleus of **5** was taken from the crystal structure of **3**. In all cases the piperidine ring was studied first (increments of 3°) and, subsequently, the ester group torsional angles of the lowest energy axial and equatorial conformations were scanned (increments of 5°), allowing an energy window of 10 kcal mol^{-1}. For compounds **7–11**, the search was performed on the three ester bonds plus the three bonds originating from the 'acetyl' C atom (increments of 10°). Spiro derivatives **4** and **13** were studied as described for the templates. The oxathiolane compound **13** was built from the structure of **2**, by changing the ethereal O atom into an S atom. The same procedure of simply modifying **2** was not allowed for compound **4** because of the steric repulsion arising from a van der Waals contact between the H atom in position 1 of the fluorenyl nucleus and the equatorial H atom in position 3 of the piperidine ring. This was caused by puckering of the oxodioxolane ring and implied the rebuilding of the ring in a planar conformation. The molecule was studied as described above, starting from the planar geometry.

All the structures representing low energy conformations were first minimized with the Tripos force field (MAXIMIN2) and then fully optimized with the AM1 program.[28] MNDO[29] was used for the optimization of **13**, due to the lack of parameterization of the S atom in the AM1 version presently available.

'Active' conformations of compounds **1** and **5–12** were SEARCHed by rotating the torsional angles of the linear ester linkage; increments of 5° over the range 0–360° and an energy window of 50 kcal mol^{-1} were set up. Constraints were imposed on the distances between the N atom and the carbonyl O atom and between the N atom and each of the centroids of the phenyl rings. Two sets of distance ranges were used, corresponding to the A and B pharmacophoric frames (see Table 2); a tolerance of ±1.0 Å was associated to each distance constraint. Low energy conformations previously located were used as starting geometries for these searches and variable numbers of conformations were obtained matching the constraints. Among the found conformations, one or two were selected for each compound and designated as 'active' conformations, according to the criteria of good fit to the A and B frames and energetic accessibility. The rmsd of the fit was calculated for the atoms involved in the receptor binding by comparing (FIT procedure) each selected structure and the pharmacophoric frame; each putative active conformation was optimized (AM1) prior to fitting. The lowest energy flipped conformations of the spiro derivatives **4** and **13** were considered as their active conformations.

Acknowledgment

This work was supported by a grant from MURST.

References and Notes

1. Hammer, R.; Berrie, C. P.; Birdsall, N. J. M.; Burgen, A. S. V.; Hulme, E. C. *Nature* **1980**, *283*, 90.

2. Melchiorre, C.; Cassinelli, A.; Quaglia, W. *J. Med. Chem.* **1987**, *30*, 201.

3. Melchiorre, C.; Quaglia, W.; Picchio, M. T.; Giardinà, D.; Brasili, L.; Angeli, P. *J. Med. Chem.* **1989**, *32*, 79.

4. Melchiorre, C. *Med. Chem. Rev.* **1990**, *10*, 327.

5. Melchiorre, C.; Bolognesi, M. L.; Chiarini, A.; Minarini, A.; Spampinato, S. *J. Med. Chem.* **1993**, *36*, 3734.

6. Barlow, R. B.; Berry, K. J.; Glenton, P. A. M.; Nikolaou, N. M.; Soh, K. S. A. *Br. J. Pharmacol.* **1976**, *58*, 613.

7. Bonner, T. I. *Trends Neurosci.* **1989**, *12*, 148.

8. Tumiatti, V.; Recanatini, M.; Minarini, A.; Melchiorre, C.; Chiarini, A.; Budriesi, R.; Bolognesi, M. L. *Il Farmaco* **1992**, *47*, 1133.

9. This compound was included in a general formula reported by: Nakanishi, M.; Arimura, K.; Ao, H. *Chem. Abstr.* **1973**, *78*, 124567v. However, it was tested only in guinea pig ileum.

10. Belleau, B.; Monkovic, I. *Chem. Abstr.* **1971**, *74*, 12987t.

11. Becker, H.; Bistrzycki, A. *Chem. Ber.* **1914**, *47*, 3149.

12. Barlow, R. B.; Shepherd, M. K. *Br. J. Pharmacol.* **1986**, *89*, 837.

13. Barlow, R. B.; Shepherd, M. K. *Br. J. Pharmacol.* **1985**, *85*, 427.

14. Larsen, A. A.; Wayne Ruddy, A.; Elpern, B.; MacMullin, M. *J. Am. Chem. Soc.* **1949**, *71*, 532.

15. Sabatino, P.; Recanatini, M.; Tumiatti, V.; Melchiorre, C. *Acta Cryst.* **1994**, *C50*, 640.

16. Desiraju, G. R. *Acc. Chem. Res.* **1991**, *24*, 290, and references therein.

17. Arunlakshana, O.; Schild, H. O. *Br. J. Pharmacol.* **1959**, *14*, 48.

18. Tallarida, R. J.; Cowan, A.; Adler, M. W. *Life Sci.* **1979**, *25*, 637.

19. Angeli, P.; Giannella, M.; Pigini, M.; Gualtieri, F.; Teodori, E.; Valsecchi, B.; Gaviraghi, G. *Eur. J. Med. Chem.* **1986**, *20*, 517.

20. Marshall, G. R.; Barry, C. D.; Bosshard, H. E.; Dammkoehler, R. A.; Dunn, D. A. In: *Computer-Assisted Drug Design*, p. 205, Olson, E. C.; Christoffersen, R. E., Eds; American Chemical Society; Washington, DC, 1979.

21. Hansch, C.; Leo, A. J. *Substituent Constants for Correlation Analysis in Chemistry and Biology*, Wiley Interscience; New York, 1979.

22. Anisotropic temperature factor parameters, atomic coordinates, individual bond lengths and angles are available from one of the authors (PS).

23. Sheldrick, G. M. *Acta Cryst.* **1990**, *A46*, 467.

24. Sheldrick, G. M. *J. Appl. Cryst.* **1994**, in press.

25. SYBYL Molecular Modeling System (Version 5.5), Tripos Ass., St. Louis, MO.

26. NITRO (Version 6.0), Tripos Ass., St. Louis, MO.

27. Barlow, R. B.; Howard, J. A. K.; Johnson, O.; Sanders, T. M. *Acta Cryst.* **1987**, *C43*, 671.

28. Dewar, M. J. S.; Zoebisch, E. G.; Healy, E. F.; Stewart, J. J. P. *J. Am. Chem. Soc.* **1985**, *107*, 3902.

29. Dewar, M. J. S.; Thiel, W. *J. Am. Chem. Soc.* **1977**, *99*, 4899.

(*Received in U.S.A.* 9 *November* 1994; *accepted* 16 *December* 1994)